

## Compressive-Stress-Induced Formation of Thin-Film Tetrahedral Amorphous Carbon

D. R. McKenzie, D. Muller, and B. A. Pailthorpe

*School of Physics, University of Sydney, Broadway, NSW 2006, Australia*

(Received 3 December 1990)

Thin tetrahedrally coordinated amorphous carbon (*ta*-C) films have been grown using a filtered vacuum arc. *ta*-C is a new allotrope of carbon whose existence was previously thought to be unlikely. A model is proposed which accounts for the formation and structure of these films on the basis of the compressive stress generated by the shallow implantation of carbon ions. An optimal range of beam energies between 15 and 70 eV, a high film stress, and a graphitic surface are predicted and confirmed by experimental evidence. Computer simulation of the growth confirms that high compressive stress is generated by impact energies in this range.

PACS numbers: 81.30.-t, 34.90.+q, 61.14.Rq, 71.45.Gm

Carbon exists in two major allotropic forms, graphite and diamond. The diamond allotrope consists of fourfold-coordinated carbon atoms ( $sp^3$  hybrids). In graphite, the atoms are threefold coordinated as  $sp^2$  hybrids, forming planes of six-member rings. For in-plane distortions graphite has great strength but bonding between the planes is solely due to van der Waals interactions, making it both soft and a good lubricant. Graphite is thermodynamically stable with respect to diamond at standard temperature and pressure (STP). Perhaps the most common carbon structure is amorphous carbon (*a*-C), a disordered form of graphite [1]. Experimental evidence suggests that well over 80% of the atoms in *a*-C thin films are  $sp^2$  hybrids [2,3]. Diamondlike hydrogenated carbons (*a*-C:H) have an increasing fraction of  $sp^3$  sites as the hydrogen content increases but the fraction of carbon-carbon  $sp^3$  bonds changes little and the hardness of the film decreases as the hydrogen atoms interrupt the carbon network [4,5].

An amorphous form of diamond, i.e., disordered tetrahedral carbon (*ta*-C), was previously thought to be unlikely to exist [4] because of the bonding constraints imposed on the carbon network, although such a structure is present in amorphous silicon and germanium. In addition, the  $sp^2$  hybrid has a lower energy configuration than the  $sp^3$  at STP in carbon while the opposite is true for silicon and germanium [6].

In this Letter we present evidence which confirms the existence of this amorphous form of diamond which we show is structurally similar to *a*-Ge and *a*-Si. This disordered tetrahedral carbon is almost entirely  $sp^3$  bonded and has a density, hardness, and electrical resistivity near that of natural diamond. We present evidence for the mechanism of formation of tetrahedral amorphous carbon being the high compressive stress generated during deposition driving the effective pressure and temperature conditions to a point well inside the diamond stable zone as defined by the Berman-Simon line [7].

Soviet groups (Aksenov, Belous, Padalka, and Khoroshikh [8]) were the first to produce hard carbon coatings deposited from the filtered plasma stream of a vacuum arc running on a graphite cathode. Our studies of the small-angle electron scattering [9], electron-energy-loss

spectroscopy (EELS) [10], and radial distribution analysis [2,11] of such films showed an amorphous structure in which the fraction of  $sp^3$  hybridized carbon atoms was approximately 0.9. This material showed high densities of approximately 2.9 g/cm<sup>3</sup> as determined by a flotation method, and a high microhardness [6000–13000 Hv (Vickers microhardness) compared with 12000 Hv for diamond] with an elastic recovery [12].

First, structural evidence is presented to confirm the existence of *ta*-C. Structure in an amorphous material is essentially of a short-range nature and is best described by a radial distribution function which gives a measure of the most probable distances between atoms. Here we use the reduced density function:

$$G(r) = 4\pi r [\rho(r) - \rho_0], \quad (1)$$

where  $\rho(r)$  is the average density at a distance  $r$  from an atom center and  $\rho_0$  is the density averaged over the complete specimen.  $G(r)$  is obtained by collecting an energy-filtered electron-diffraction pattern  $I(s)$  using techniques described previously [11] and Fourier-sine transformation:

$$G(r) = 8\pi \int_0^{s_{\max}} s \left( \frac{I(s) - Nf^2}{Nf^2} \right) D(s) \sin(2\pi sr) ds, \quad (2)$$

where  $s = 2(\sin\theta)/\lambda$ ,  $2\theta$  is the scattering angle,  $\lambda$  is the de Broglie wavelength of the electrons,  $f$  is the atomic scattering factor of a single atom, and  $D(s)$  is a damping function, in this case  $\text{sinc}(s/s_{\max})$ . The resolution of the data is determined by  $s_{\max}$ , where  $s_{\max} = 4.2 \text{ \AA}^{-1}$ .

The  $G(r)$  provides two independent means of distinguishing threefold-coordinated from fourfold-coordinated carbon. First, the bond length is given by the nearest-neighbor distance (1.42 Å for graphite, 1.54 Å for diamond, and  $1.53 \pm 0.01 \text{ \AA}$  for *ta*-C). Second, the bond angle can be obtained from the ratio of the first- and second-neighbor distances as  $\theta = 2\sin^{-1}(r_2/2r_1)$  ( $109.47^\circ$  for diamond,  $120^\circ$  for graphite, and  $110 \pm 0.5^\circ$  for *ta*-C). Similar results have been obtained from neutron scattering, although with a lower resolution ( $s_{\max} = 2.4 \text{ \AA}^{-1}$ ), giving a bond angle of  $110.3^\circ$  and a coordination number of 3.7 [13,14]. Both the bond length and bond angle are consistent with 92%  $sp^3$  hybridization in *ta*-C.

The structure of amorphous diamond is analogous to that of amorphous silicon or germanium, both being well described by random tetrahedral networks such as that of Polk and Boudreaux [15]. In such a network any three-fold-coordinated material could be regarded as an impurity rather than a necessary component. Figure 1 shows the  $G(r)$  for *ta*-C. For comparison the  $G(r)$  for amorphous germanium is also shown, but with the distance axis rescaled so that nearest-neighbor distances coincide. Overall the agreement is excellent over the complete distance scale shown. Note in both cases the flat region between the second and third peaks which is characteristic of all amorphous tetrahedrally bonded semiconductors and is caused by a uniform distribution of the dihedral angles. Small differences in the relative widths of the first and second peaks between *ta*-C and amorphous germanium are attributed to the greater bond-angle "stiffness" in  $sp^3$  carbon than in  $sp^3$  germanium [2,9].

A study of the surface plasmon excitation shows that the surface of the material is almost entirely  $sp^2$  carbon as predicted. Since the overall fraction of  $sp^3$  sites in the film is about 0.9 as determined by the  $G(r)$  and carbon *K*-edge [10] analyses, this implies that the fraction of  $sp^3$  sites in the interior of the film must be higher than 0.9 as would be expected for a random tetrahedral network.

We consider the determination of  $G(r)$  the strongest evidence for the tetrahedral nature of these films. Not only does the  $G(r)$  provide a measure of the bond length and bond angle but also a description of the microstructure, which is shown to be remarkably similar to that of other amorphous semiconductors. The EELS, plasmon, and density measurements show the films have a very high fraction of  $sp^3$ -bonded material mixed with a very small fraction of  $sp^2$  material in an unspecified way.

The  $C^+$ -ion energy from our filtered arc source, described in detail elsewhere, has a distribution peaking at 22 eV [12] and this energy was varied at the substrate [a silicon (100) wafer] by biasing so that the most probable energy could be varied from 0 to 1000 eV. Care was taken to supply sufficient current to enable the voltage to be maintained during operation of the vacuum arc. Typical-

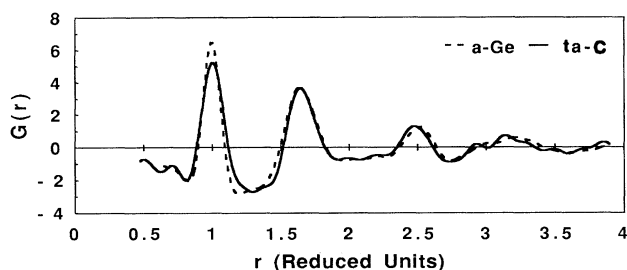


FIG. 1. The reduced density function for tetrahedral amorphous carbon compared with that for amorphous germanium. The distance scale is obtained by dividing the actual distance by the nearest-neighbor distance.

ly a 40-nm film could be deposited in 1 min.

The intrinsic stress in the deposited film was measured by determining the substrate curvature interferometrically using the method of Newton's rings. The intrinsic stress is that left after the thermal stress ( $\sim 0.7$  GPa) has been accounted for. If the radii of curvature of the substrate before and after deposition are  $R_0$  and  $R$ , respectively, then the film stress is given by

$$\sigma = \frac{Y}{6(1-\nu)} \frac{t_s^2}{t} \left( \frac{1}{R} - \frac{1}{R_0} \right), \quad (3)$$

where  $Y$  and  $\nu$  are the Young's modulus and Poisson's ratio of the silicon substrate of thickness  $t_s$ . The film thickness  $t$  was measured using a stylus profilometer.

For each specimen we determined the plasmon energy by means of electron-energy-loss spectroscopy. We found that this energy correlates well with the fraction of  $sp^3$  carbon as determined by the nearest-neighbor distances and bond angles obtained from the  $G(r)$  function. High plasmon energies (29.5 to 30.5 eV) coincided with almost complete tetrahedral bonding of the carbon, as deduced from the  $G(r)$  function. The plasmon energy also may be used to measure film density using the standard free-electron relation:

$$\omega_p^2 = ne^2/\epsilon_0 m, \quad (4)$$

where  $E_p = \hbar \omega_p$  is the plasmon energy and  $n$  is the number of electrons per unit volume taking part in plasma oscillations (assumed to be 4.0 per atom). For low- $sp^3$ -fraction amorphous-carbon films  $E_p$  is typically 24–25 eV while that of graphite is 27 eV. The calculated plasmon energy of diamond, assuming a density of 3.51 g/cm<sup>3</sup>, is 31 eV while the measured peak is at 33 eV. In diamond, distortion of the plasmon peak resulting from selection rules applying to a crystal produces a value higher than expected. For both silicon and germanium, the plasmon energy of the crystalline form is higher than that of the amorphous form [16,17]. By comparison, evaporated  $sp^2$ -rich amorphous carbon has a density about 80% that of graphite (1.8–2.0 vs 2.26 g/cm<sup>3</sup>) [1,4] which is similar to the ratio of densities between the tetrahedral amorphous carbon (2.9 g/cm<sup>3</sup>) and that of diamond (3.51 g/cm<sup>3</sup>).

Figure 2 shows the dependence of both the film stress  $\sigma$  and the plasmon energy on the most probable energy of the  $C^+$  incident ions. The amorphous tetrahedral network structure is produced for ion energies greater than about 15 eV but beyond about 50 eV there is a progressive reduction in plasmon energy and hence fraction of  $sp^3$  carbon. Significantly, there is a close correlation between high plasmon energy and high compressive film stress. The significance of this is best shown by plotting the effective hydrostatic pressure  $P$  resulting from the film stress on the carbon  $P$ - $T$  diagram (Fig. 3). The diamond region is entered for energies greater than about 15 eV and is exited for energies greater than about 1000 eV, in agreement with the observations of local structure.

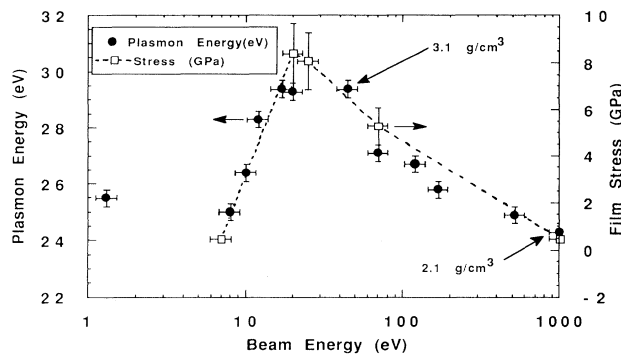


FIG. 2. Plots of the stress and plasmon energy for films deposited at various carbon ion energies.

The effective hydrostatic pressure is obtained using the reduction of any deformation into a hydrostatic compression plus a shear distortion [18]. It is readily shown [18] that the hydrostatic component  $P$  of a biaxial compressive stress  $\sigma$ , as applied to a thin film by the substrate when the film is under compressive stress, is given by  $P = \frac{2}{3} \sigma$ , where  $\sigma$  is the value of the compressive stress as determined from the curvature of the substrate.

The upper surface of the film is a free surface and stress there can be relieved by the movement of surface atoms. The stress will drop from its bulk value inside the film to zero at the surface over some characteristic length, crossing the Berman-Simon line. Consequently, graphite will be the stable phase on the immediate surface and the model predicts a thin surface layer of  $sp^2$  material even when the conditions inside the film are well inside the diamond zone. Surface plasmon measurements confirm this prediction.

In order to understand the origins of the compressive stress, we carried out a molecular-dynamics (MD) study of the film growth using a modified Stillinger-Weber potential [19,20]. The interaction potential was based on reparametrization of the Stillinger-Weber potential using a Hartree-Fock energy calculation for small tetrahedrally coordinated carbon clusters which has been discussed previously [19,20]. This potential was tested in a 512-atom simulation which predicted a bulk modulus for diamond at 500 K of 460 GPa, compared to the experimental value of 442 GPa and an *ab initio* quantum calculation of 433 GPa [6]. The predicted liquid density (at 5400 K and 90 kbar) was 17% less than the solid, consistent with the results of Galli, Martin, Car, and Parrinello [21].

The initial nucleation of carbon on the silicon substrate was assumed to have already taken place in the form of a complete layer of cubic diamond  $3 \times 3$  unit cells across, having the (111) direction normal and being five atomic layers deep. The base layer was rigidly fixed. The trajectories of the incident atom and the 320 atoms on the substrate with which it interacts were followed at time steps of 0.027 fs. A spread of impact parameters was used to give the effect of a beam of neutralized ions. Energy was

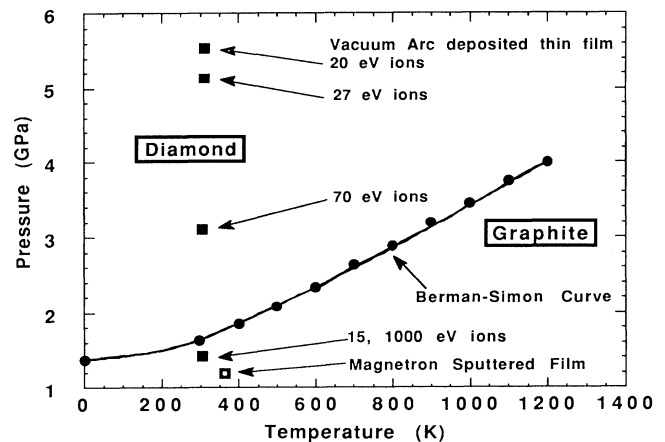


FIG. 3. The  $P$ - $T$  phase diagram for carbon showing the Berman-Simon curve. The solid squares are obtained from the measured compressive stresses in vacuum-arc-deposited films. Also shown is the result for a dc-magnetron-sputtered film.

removed at the substrate interface in one of three ways. First, the fourth subsurface layer was thermostated to the substrate temperature  $T_s$  by periodic rescaling of all its atomic velocities modulated with a random phase, i.e., a random thermostat. Second, an adiabatic simulation [22], in which all the energy released during an atomic deposition was used to heat the substrate, produced qualitatively similar results to our model thermostats and so confirmed that no artifacts were introduced. Finally, the thermostated layer was maintained at 0 K, corresponding to the fastest physically possible heat removal mechanism (to a heat sink at absolute zero). This produced essentially identical results to the random thermostat so that the latter was adopted here. The atomic motions were followed for 3–5 ps so that the heat extraction rate was typically  $10^{11}$  W/m<sup>2</sup> which is substantially greater than can be realized experimentally. This problem is shared with MD simulations [23–25] of *a*-Si which nevertheless predict structures which compare favorably with available experimental data.

The average compressive stress was calculated after the incident energy had been almost completely dissipated (within 1–5 ps) by evaluating the force acting across the  $x$ - $z$  and  $y$ - $z$  planes in the deposited film. The dependence of the compressive stress is presented in Fig. 4 and shows the same form as the experimental data, that is, a rapid rise at energies of approximately 20 eV and a slow decline for energies above 60 eV.

By following the atom trajectories, an overall picture could be obtained of the processes occurring in three energy bands. For energies less than about 20 eV, the incident atom is reflected without any change to the structure of the deposited layers. For intermediate energies of 20–60 eV the incident atoms penetrate the subsurface layer and induce local compression. At higher energies

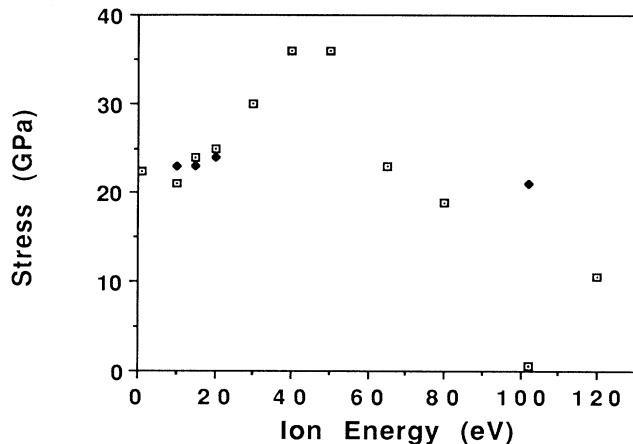


FIG. 4. The molecular-dynamics result for the compressive stress developed in a thin diamond film as a function of the impact energy. Results for two different impact parameters are shown.

(80–100 eV), the incident atoms penetrate more deeply and induce knockon collisions which displace underlying atoms even deeper into the film. Variation of the impact parameter does not have a significant effect on the results.

This behavior might be regarded as a “thermal spike” [26,27] in which localized melting and rapid chilling of a small region occurs, leaving it in a stressed state. With increasing energy the impact creates a region large enough to flow and thereby relieve stress.

Lifshitz, Kasi, and Rabalais [28] have discussed an additional mechanism for the promotion of  $sp^3$  bonding by the preferential displacement of  $sp^2$  atoms by the impact of incoming ions. We would also expect this mechanism to lead to high compressive stresses developed from the inwardly displaced  $sp^2$  atoms.

In vacuum-arc growth the tetrahedral structure of amorphous carbon is formed under conditions in which diamond is the stable phase and is therefore fundamentally different from the metastable growth of crystalline diamond by chemical-vapor deposition under reduced pressure. An important practical difference is the much higher deposition rate for stable growth and a lower substrate temperature. The model of the stress-induced growth of tetrahedral amorphous carbon should also apply to any material having more than one phase in the pressure ranges which can be accessed by the generation of compressive stress. In particular, we predict that cubic boron nitride could be produced under conditions which lead to a high compressive stress. Filtered-vacuum-arc deposition should prove to be a useful method of accessing high-compressive-stress regimes because of its narrow and controllable energy distribution and high flux rates.

Valuable discussions with D. J. H. Cockayne and R. E. Collins are gratefully acknowledged.

[1] J. Robertson, *Adv. Phys.* **35**, 317 (1986).

[2] D. C. Green, D. R. McKenzie, and P. B. Lukins, in *Prop-*

*erties and Characterisation of Amorphous Carbon Films*, edited by J. J. Pouch and S. A. Alterovitz (Trans Tech, Nedermansdorf, 1990), Vol. 103.

[3] F. Li and J. Lannin, *Phys. Rev. Lett.* **65**, 1905 (1990).

[4] J. C. Angus and C. C. Hayman, *Science* **241**, 913 (1988).

[5] F. Jansen, M. Machonkin, S. Kaplan, and S. Hark, *J. Vac. Sci. Technol. A* **3**, 605 (1985).

[6] M. T. Yin and M. L. Cohen, *Phys. Rev. B* **24**, 6121 (1981); **29**, 6996 (1984).

[7] R. Berman and F. Simon, *Z. Elektrochem.* **59**, 333 (1955).

[8] I. I. Aksenov, V. A. Belous, V. G. Padalka, and V. M. Khoroshikh, *Fiz. Plazmy* **4**, 758 (1978) [*Sov. J. Plasma Phys.* **4**, 425 (1978)].

[9] D. R. McKenzie, P. J. Martin, S. B. White, Z. Liu, W. G. Sainty, D. J. H. Cockayne, and D. M. Dwarthe, in *Proceedings of the European Materials Research Society Meeting, Strasbourg, June 1987* (Les Editions de Physique, Paris, 1987), Vol. 17, p. 203

[10] S. D. Berger, D. R. McKenzie, and P. J. Martin, *Philos. Mag. Lett.* **57**, 285 (1988).

[11] D. J. H. Cockayne and D. R. McKenzie, *Acta Crystallogr.* **44**, 870 (1988).

[12] P. J. Martin, S. W. Filipczuk, R. P. Netterfield, J. S. Field, D. F. Whitnall, and D. R. McKenzie, *J. Mater. Sci. Lett.* **7**, 410 (1988).

[13] D. R. McKenzie, D. Muller, B. A. Pailthorpe, Z. H. Wang, E. Kravtchinskaiia, D. Segal, P. B. Lukins, P. D. Swift, P. J. Martin, G. Amaratunga, P. H. Gaskell, and A. Saeed, in *Proceedings of Diamond Films '90, First European Conference on Diamond and Diamond-like Carbon Coatings, Crans-Montana, Switzerland, 17–19 September 1990* [*Surf. Coat. Technol.* (to be published)].

[14] P. H. Gaskell, A. Saeed, P. Chieux, and D. R. McKenzie (to be published).

[15] D. E. Polk and D. S. Boudreaux, *Phys. Rev. Lett.* **31**, 92 (1973).

[16] R. F. Egerton, *Electron Energy Loss Spectroscopy in the Electron Microscope* (Plenum, New York, 1986).

[17] D. R. McKenzie, P. S. Turner, and D. J. H. Cockayne, *Phys. Status Solidi (a)* **96**, 67 (1986).

[18] L. D. Landau and E. M. Lifshitz, *Theory of Elasticity* (Pergamon, London, 1959).

[19] B. A. Pailthorpe and P. Mahon, *Thin Solid Films* **193/194**, 34 (1990).

[20] P. Mahon, B. A. Pailthorpe, and G. Bacskey, *Philos. Mag. B* (to be published).

[21] G. Galli, R. M. Martin, R. Car, and M. Parrinello, *Phys. Rev. Lett.* **62**, 555 (1989); **63**, 988 (1989).

[22] F. H. Stillinger and T. A. Weber, *Phys. Rev. Lett.* **62**, 2144 (1989).

[23] M. Schneider, I. K. Schuller, and A. Rahman, *Phys. Rev. B* **36**, 1340 (1987).

[24] E. T. Gawlinski and J. D. Gunton, *Phys. Rev. B* **36**, 4774 (1987).

[25] M. D. Kluge, J. R. Ray, and A. Rahman, *Phys. Rev. B* **36**, 4234 (1987).

[26] C. Weissmantel, *Thin Solid Films* **92**, 55 (1982).

[27] F. Seitz and J. S. Koehler, *Progress in Solid State Physics* (Academic, New York, 1957), Vol. 2, p. 30.

[28] Y. Lifshitz, S. R. Kasi, and J. W. Rabalais, *Phys. Rev. Lett.* **62**, 1290 (1989).